Coprime-frequencied sinusoidal modulation for improving the speed of computational ghost imaging with a spatial light modulator

Quan Li (黎 全)[1,2], Zhentao Duan (段振涛)[1,2], Huizu Lin (林惠祖)[1,2], Shaobo Gao (高少博)[1,2], Shuai Sun (孙 帅)[1,2], and Weitao Liu (刘伟涛)[1,2,*]

[1]*College of Science, National University of Defense Technology, Changsha 410073, China*
[2]*Interdisciplinary Center of Quantum Information, National University of Defense Technology, Changsha 410073, China*
**Corresponding author: wtliu@nudt.edu.cn*

Received July 21, 2016; accepted September 30, 2016; posted online November 9, 2016

Correlation imaging is attracting more and more attention as a novel imaging technique taking advantage of the high-order coherence of light fields. To reconstruct an image of the object, many frames of different speckle patterns are required. Therefore, the speed of imaging is strongly limited by the speed of the refreshing rate of the light field. We propose a coprime-frequencied sinusoidal modulation method for speckle pattern creation using a spatial light modulator in a computational ghost imaging system to increase the speed of imaging. The performance of the proposed method is discussed as well.

OCIS codes: 110.6150, 030.6600, 110.2945.
doi: 10.3788/COL201614.111103.

Ghost imaging, also called correlation imaging, offers a novel imaging method, being able to image without any spatially resolved detector or even with only a single-pixel detector. A typical correlation imaging system consists of two arms of light. One arm, the reference arm, is equipped with a spatially resolved detector (such as a CCD camera) to record the intensity distribution of the light field. While the other arm, the object arm, is equipped with a bucket detector, which collects the transmitted or reflected light from the object. The light beams in two arms are usually created by separating the beam from the light source into two, such that the intensity distributions on the two arms are strongly correlated. After a variety of speckle patterns are sequentially illuminated onto the object, an image of the object can be obtained by calculating the correlation function (over all those frames of patterns) between the signals from the CCD and the bucket detector[1–9]. In such a system, if the patterns at the plane of the object can be actively controlled and precisely calculated, the spatially resolved detector and the reference arm are no longer required. This idea is called computational ghost imaging[10,11], and it has been experimentally demonstrated using a spatial light modulator (SLM) to transform a laser into temporal-spatially fluctuating speckle patterns, with a schematic diagram of the typical setup shown in Fig. 1. This proposal can greatly simplify the system and speed up the imaging process, since the experimental limitation of the sampling rate of the CCD is eliminated. Since ghost imaging promises prospective applications, it attracts more and more attention, considering its practical application and enhancement on the performance of ghost imaging systems[12–27].

In most occasions, the series of speckle fields are regulated by an SLM loading different random phases $\phi(\xi,\eta)$ at positions (ξ,η) of a plane wave light field. So the light field regulated by the SLM can be written as $E_0(\xi,\eta)=e^{i\phi(\xi,\eta)}$, assuming that the amplitude of the light field is unity. Then the speckle patterns at the far field can be calculated according to the Huygens–Fresnel approximation[28,29]. The speckle field on the plane of the object at a distance of z will be

$$E(x,y)=\frac{e^{ikz}}{i\lambda z}\iint_{-\infty}^{+\infty}E_0(\xi,\eta)e^{\frac{ik}{2z}[(x-\xi)^2+(y-\eta)^2]}\mathrm{d}\xi\mathrm{d}\eta, \quad (1)$$

where λ is the wavelength of the laser and k is the wave vector. The propagation of light from (ξ,η) on the source plane to (x,y) on the object plane is described by the pulse response function, and the field distribution on the object plane is determined by the whole phase mask on the source plane.

From Eq. (1), the speckle fields show the character of random fluctuations in the spatial and temporal domains, since $\phi(\xi,\eta)$ is randomly set. This kind of fluctuation is necessary for correlation imaging. Theories and experiments indicate that the distribution of speckle fields is one of the dominant factors for correlated imaging, and a series of well-designed speckle fields can be helpful for improving the quality of images[30–33].

On the other hand, because of the random fluctuations, many frames of different patterns are required to retrieve the image. Typically, the more complex the object is, the

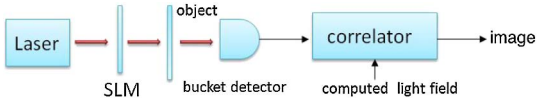

Fig. 1. Schematic diagram of a typical setup for computational ghost imaging with an SLM.

more varieties of speckle patterns are required. Therefore the shortest time to obtain a ghost image will be limited by the refreshing rate of the speckle patterns. Or, increasing the refreshing rate of the speckle patterns will be an effective way to improve the speed of correlated imaging. A high imaging speed can be vital if the object to be imaged is in motion. In addition, considering practical utility, environment factors such as temperature, humidity, atmospheric turbulence, and atmospheric scattering will affect the quality of ghost images, which are usually changing over time. A possible way to reduce such influence is to accomplish the imaging process as soon as possible, which also requires a high refreshing rate of the speckle fields. Given that speckle fields can be calculated by light fields from the light source, it is important to explore better and faster schemes for the regulation of light sources.

Considering computational ghost imaging with an SLM, the refreshing rate of the speckle patterns is determined by the refreshing rate of the random phase mask loaded on the SLM, which is typically refreshed frame by frame. That means only after all the pixels of the SLM are refreshed, the next phase mask can be loaded. This turns out to be the main limitation of the refreshing rate of speckle patterns. However, the response speed of each pixel on the SLM could be much faster if we control those pixels independently. At the same time, when controlling the phase of every pixel, it is reasonable that the response of the pixel will be more stable if the input is a smooth signal, such as sinusoidal signal, rather than a random modulation signal. What is more, a sinusoidal modulation signal can be much easier and more precisely generated compared to random modulation signals.

Here, we propose to control every pixel of the SLM with a sinusoidal signal independently to increase the refreshing rate of the speckle patterns. The sinusoidal signals for different pixels are sets of different frequencies so that the phase differences between the pixels will vary with time, therefore also the generated speckle patterns at the object plane. Without a loss of generality, the frequencies of all the sinusoidal signals are considered to be integers, for convenience. Additionally, it is noticed that the speckle fields will show temporal periodicity due to the periodicity of the sinusoidal signals. The frequency of the periodic speckle field is the largest common divisor of those of the sinusoidal signals. Meanwhile, the entire imaging process should be finished within one period. Otherwise, speckle fields will be repeated, and the corresponding results of the bucket detector will also be repeated, thus giving no more information on the object. So, frequencies should be set to make the fluctuation of the speckle patterns as random as possible, or to make the period of the speckle fields long enough such that there are enough different speckle patterns within one period. To achieve this, the frequency of all those different sinusoidal signals are set to be coprime. In this case, the temporal period of the speckle fields will be 1 s.

Since the phase loaded on each pixel of the SLM is varying with time, a pulsed laser will be better than a continuous wave in practice to achieve high-quality images. By setting the pulse duration short enough, the phase loaded on each pixel can be taken as constant during the pulse. At the same time, the time interval between two pulses should be long enough such that the modulated phases for these two pulses are not similar to each other. Under this situation, one pulse provides one frame of speckle pattern, thus the refreshing rate of the speckle fields is identical to the repetitive frequency of the laser pulse. Therefore, the refreshing rate of the speckle patterns is no longer directly limited by the refreshing rate of the SLM.

Specifically, the sinusoidal signal loaded on each pixel of the SLM can be written as

$$\phi(\xi,\eta,t) = A\,\sin[2\pi f(\xi,\eta)t] + \phi_0(\xi,\eta), \tag{2}$$

where $f(\xi,\eta)$ is the modulation frequency on pixel (ξ,η) and ϕ_0 is a randomly chosen initial phase. $A \geq \pi$ assures the loaded phase occupying the whole interval $\{-\pi,\pi\}$, $\bmod 2\pi$. Assume the first pulse is lit on the SLM at time $t=0$, then the nth pulse will be there at time

$$t = \frac{n-1}{f_0}, \tag{3}$$

with f_0 being the repetitive frequency of the pulse and also the sampling rate of imaging. Since the pulses are uniformly distributed over time and the sine function is a nonlinear function, the distribution of the loaded phase will not be uniform in the interval of $\{-\pi,\pi\}$, $\bmod 2\pi$, as is that of random modulation. For ghost imaging, random modulation usually provides a better imaging quality in which the modulated phase on each pixel complies with uniform distribution. If the amplitude of the sinusoidal function is higher than π, those phases located out of $(-\pi,\pi)$ will be divided by 2π, with the remainder treated as a loaded phase. That is, the outside part will be remapped into the interval of $(-\pi,\pi)$. Therefore, the phase distribution is related to the amplitude, since the occupation of such phases beyond $(-\pi,\pi)$ is related to the amplitude. By changing the amplitude A of the sinusoidal signal, the phase distribution can be optimized to be closer to a uniform distribution. As an example, histograms of the modulation phase $\phi(\xi,\eta)$ for $A=\pi$ and $A=1.87\pi$ are shown in Fig. 2, which shows that the distribution for the case of 1.87π is better than for that of π.

Then the light field of the nth pattern on the object plane can be calculated according to the Huygens–Fresnel approximation as

$$E(x,y;n) = \frac{e^{ikz}}{i\lambda z}\iint_{-\infty}^{+\infty} e^{iA\,\sin[2\pi f(\xi,\eta)(n-1)/f_0]+i\phi_0(\xi,\eta)} \times e^{\frac{ik}{2z}[(x-\xi)^2+(y-\eta)^2]}\mathrm{d}\xi\mathrm{d}\eta. \tag{4}$$

It can be inferred from Eq. (4) that the speckle fields on the object have the character of random spatial intensity

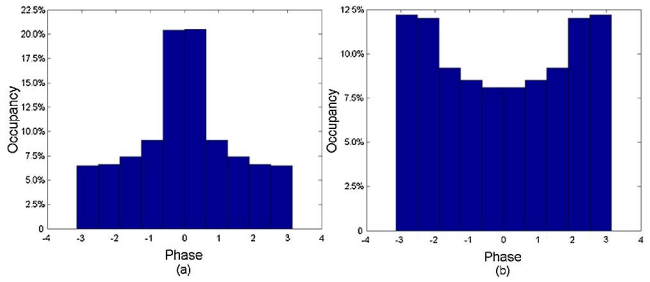

Fig. 2. Histogram to show the phase distribution. For the left one, the amplitude of the sinusoidal function is $A = \pi$, and for the right one $A = 1.87\pi$.

fluctuations, since for each light pulse the plane wave front is modulated with a random phase mask. However, the intensity fluctuations of the speckles over time are not really random, because the phase modulation of each pixel is a temporally periodic signal. To verify that our method can work for ghost imaging, we did a numerical simulation according to a system shown in Fig. 1.

As an example, the effective size of the SLM is set to be 6.14 mm × 6.14 mm, simulated with 10 × 10 pixels. The wavelength of the laser is 1064 nm. An area of 2.4 mm × 2.4 mm at a distance of 0.5 m from the surface of the SLM is considered as the object. The size of the image is set as 100 × 100 and the amplitude of the sinusoidal function is set as $A = 1.87\pi$. An easy way to set the frequencies to be caprice is to use prime numbers. The frequencies of sinusoidal signals are chosen to be the smallest 100 prime numbers, namely, the prime numbers from 2 to 541. A binary letter "E" is used as the object in the numerical simulation. The sampling rate is set to be 2000 Hz and the number of frames is also set to be 2000. The imaging result is shown in Fig. 3(a). It is shown that our method is effective for ghost imaging, and the refreshing rate of the speckle patterns can be higher than the highest modulation frequency on pixels of the SLM. For comparison, we also simulated the case that each pixel of the SLM is modulated with a random signal, and the imaging result is shown in Fig. 3(b). Also, the case that loading sinusoidal modulations of different but non-coprime frequencies is shown in Fig. 3(c). From Fig. 3, the image quality of coprime-frequencied modulation is better than that of the non-coprime case, and is very close to that of random modulation. For the non-coprime case, the modulated pixels are no longer entirely independent and the randomness of speckle patterns becomes worse than that of the coprime case, thus the image quality is not as good.

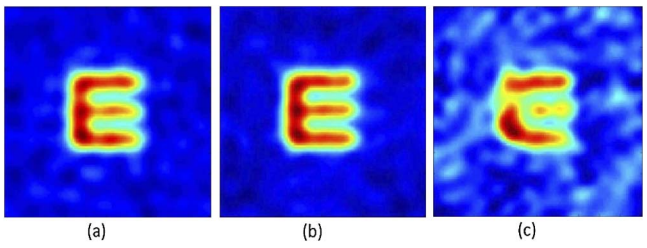

Fig. 3. Ghost imaging results of a binary object, with the phase modulation loaded on the SLM set to be (a) coprime-frequencied sinusoidal, (b) random modulation signal, and (c) sinusoidal signals of the non-coprime different frequencies.

To estimate the performance of our method, we also measure the image quality using the mean square error (MSE) and investigate its behavior with an increasing number of frames. By changing the repetitive rate f_0 of the pulse, the number of frames can be changed and all the frames are sampled within 1 s.

A more detailed comparison between our method and random modulation is shown in Fig. 4. It is shown that the MSE of the obtained images for both cases do not show much difference, which means that the image quality of our method is very close to that of random modulation and our method can work well for ghost imaging.

At the same time, the performance of our method is related to the combination of those sinusoidal frequencies and the sampling rate. We tried four different combinations with the modulation frequencies chosen to be 100 prime numbers in four different intervals, namely, $f \in [103, 701]$, $f \in [2, 701]$, $f \in [4003, 5003]$, and $f \in [2, 5003]$. The image quality for the same object is investigate for those cases, with the results shown in Fig. 5. For those two cases of modulation frequencies not higher than 701 Hz, the curve of the MSE becomes flat when the number of frames goes high enough, which means that detection results using more frames do not offer more information on the object. The reason lies in the fact that when the sampling rate is high, the time difference between two neighboring pulses is rather small compared to the period of every sinusoidal signal, such that the difference between loaded phase masks for them as well as the difference between two speckle patterns becomes tiny. Therefore, the effective sampling rate of our method cannot be arbitrarily high.

However, it can still be more than ten times higher than the highest modulation frequency of pixels on the SLM. This is concluded by observing the beginning spot of the flat part of the MSE curve. For these two cases of

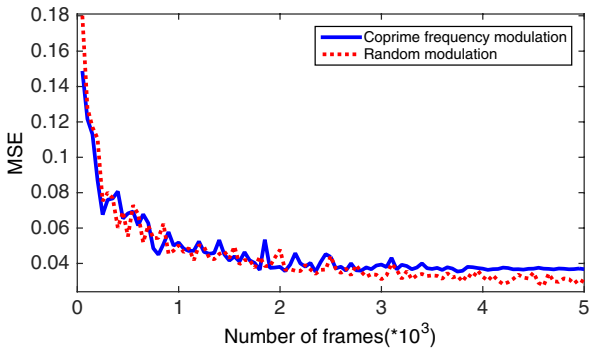

Fig. 4. Comparison between coprime-frequencied modulation and random modulation by the MSE varying with the number of frames, which does not show much difference.

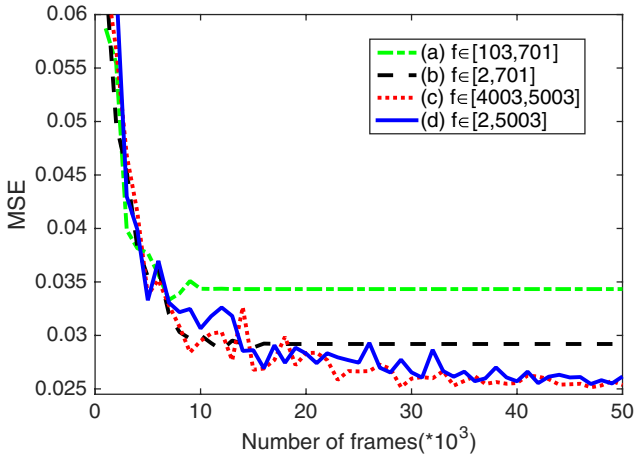

Fig. 5. Image quality measured with the MSE varying with the number of frames, with the modulation frequencies chosen to be 100 prime numbers within the interval of (a) [103, 701], (b) [2, 701], (c) [4003, 5003], and (d) [2, 5003].

low frequency, the number at the inflection point is very close to 10000, while the inflection point does not show up until 50000 frames for high modulation frequency (up to 5 kHz) cases. At the same time, increasing the separation between neighboring modulation frequencies can also help to enhance the quality of the image. From Fig. 5, it also shows that a higher modulation frequency can provide more frames of effective speckle patterns, thus a higher refreshing rate and a higher speed of ghost imaging. From the experimental view, the highest frequency f_r to which each pixel can respond is limited by the response time of the SLM. By setting the highest frequency of those coprimed frequencies as f_r, the effective sampling rate can be higher than $10f_r$.

In practice, our proposal can be demonstrated with current techniques. The only thing that might be challenging is to control every pixel of the SLM individually, which contains no difficulty in principle. The upper bound of the effective refreshing rate of the speckle patterns is tightly related to the highest frequency that can be loaded on each pixel of the SLM. In addition, the signal for every pixel is a fixed sinusoidal signal, thus the controlling part can be simplified accordingly.

In conclusion, we present and discuss a coprime-frequencied sinusoidal modulation method to increase the refreshing rate of speckle patterns, thus to increase the speed of ghost imaging based on an SLM. Every pixel of an SLM is proposed to be modulated individually with sinusoidal signals instead of random ones. The imaging quality of our method can be very close to that of random modulation. While the refreshing rate of the speckle patterns can be more than ten times higher than the highest frequency that can be responded to by each pixel of the SLM. The parameters of each modulation signal are also discussed to enhance the imaging quality.

This work was supported by the National Natural Science Foundation of China under Grant No. 11374368. W. T. Liu is also supported by the Program for New Century Excellent Talents in University.

References

1. T. B. Pittman, Y. H. Shih, D. V. Strekalov, and A. V. Sergienko, Phys. Rev. A **52**, R3429 (1995).
2. A. Valencia, G. Scarcelli, M. D. Angelo, and Y. Shih, Phys. Rev. Lett. **94**, 063601 (2005).
3. M. Zhang, Q. Wei, X. Shen, Y. Liu, H. Liu, and J. Cheng, Phys. Rev. A **75**, 441 (2006).
4. F. Ferri, D. Magatti, V. G. Sala, and A. Gatti, Appl. Phys. Lett. **92**, 261109 (2008).
5. F. Ferri, D. Magatti, A. Gatti, M. Bache, E. Brambilla, and L. Lugiato, Phys. Rev. Lett. **94**, 183602 (2005).
6. J. Cheng and S. S. Han, Phys. Rev. Lett. **92**, 1190 (2004).
7. A. Gatti, E. Brambilla, M. Bache, and L. Lugiato, Phys. Rev. A **70**, 235 (2003).
8. X. B. Song, S. H. Zhang, D. Z. Cao, J. Xiong, H. Wang, and K. Wang, Opt. Commun. **365**, 38 (2016).
9. L. Gao, S. H. Zhang, J. Xiong, S. Gan, L. J. Feng, and D. Z. Cao, Phys. Rev. A **80**, 2554 (2009).
10. Y. Bromberg, O. Katz, and Y. Silberberg, Phys. Rev. A **79**, R1744 (2009).
11. J. H. Shapiro, in *IEEE Conference on Lasers and Electro-Optics, and Conference on Quantum Electronics and Laser Science Conference. (CLEO/QELS) 2009* (IEEE, 2009), p. 1.
12. J. Y. Liu, J. B. Zhu, C. Lu, and S. S. Huang, Opt. Lett. **35**, 1206 (2010).
13. K. H. Luo, B. Q. Huang, W. M. Zheng, and L. A. Wu, Chin. Phys. Lett. **29**, 074216 (2012).
14. E. F. Zhang, W. T. Liu, and P. X. Chen, J. Opt. Soc. Am. A **32**, 1251 (2015).
15. E. F. Zhang, W. T. Liu, and P. X. Chen, Opt. Commun. **351**, 135 (2015).
16. Y. K. Xu, W. T. Liu, E. F. Zhang, Q. Li, H. Y. Dai, and P. X. Chen, Opt. Express **23**, 32993 (2015).
17. J. Cheng, Opt. Express **17**, 7916 (2009).
18. Y. Zhang, J. Shi, H. Li, and G. Zeng, Chin. Opt. Lett. **12**, 011102 (2013).
19. W. L. Gong and S. S. Han, Opt. Lett. **36**, 394 (2011).
20. D. Duan and Y. Xia, Chin. Opt. Lett. **10**, 031102 (2012).
21. C. Wang, Proc. SPIE **7658**, 76580L (2010).
22. C. Zhao, W. Gong, M. Chen, and E. Li, Appl. Phys. Lett. **101**, 141123 (2012).
23. H. C. Liu and J. Xiong, J. Opt. Soc. Am. A **30**, 956 (2013).
24. H. G. Li, D. Q. Xu, D. J. Zhang, J. J. Zhao, H. B. Wang, and J. Xiong, Opt. Commun. **326**, 115 (2014).
25. Q. Liu, K. H. Luo, X. H. Chen, and L. A. Wu, Chin. Phys. B **19**, 5 (2010).
26. X. Yao, X. Liu, W. Yu, and G. Zhai, Chin. Opt. Lett. **13**, 010301 (2015).
27. H. Ghanbarighalehjoughi, S. Ahmadikandjani, and M. Eslami, J. Opt. Soc. Am. A **32**, 323 (2015).
28. J. W. Goodman and M. E. Cox, *Introduction to Fourier Optics* (McGraw-Hill, 1968).
29. S. Sivakumar, *An Introduction to Quantum Optics: Photon and Biphoton Physics* (CRC Press 2011).
30. J. Du, W. L. Gong, and S. S. Han, Opt. Lett. **37**, 1067 (2012).
31. X. Xu, E. Li, X. Shen, and S. Han, Chin. Opt. Lett. **13**, 071101 (2015).
32. E. F. Zhang, H. Z. Lin, W. T. Liu, Q. Li, and P. X. Chen, Opt. Express **23**, 33506 (2015).
33. E. F. Zhang, W. T. Liu, and P. X. Chen, J. Opt. **17**, 085602 (2015).